



Modeling and Simulation of Photovoltaic system based grid Connected Converter with Fuzzy Logic Control

Jibilikapally Suman
P.G Student Scholar

Department of Electrical & Electronics Engineering,
Anurag Engineering College, Kodad;
Nalgonda (Dt); T.S, India.
Email:sumanjibilikapally@gmail.com

Raghu Thumu

Associate Professor

Department of Electrical & Electronics Engineering,
Anurag Engineering College, Kodad;
Nalgonda (Dt); T.S, India.
Email:raghu.eee@anurag.ac.in

Abstract—this paper focused on modeling and simulation of grid connected photovoltaic system. This work presents a fuzzy logic control based maximum power point tracking approach to enhance the efficiency and robustness of the solar photovoltaic (PV) power generation and establishes a dynamic model of grid-connected PV system by Matlab/Simulink environment which reflect the characteristics of the system accurately. Grid-connected PV system includes a PV array, dc-dc converter, fuzzy logic control based MPPT, inverter, LC filter, P-Q based inverter control, a distribution network. Improved fuzzy logic control based MPPT and P and Q based inverter control scheme provides a closed loop active and reactive power control and accurate synchronization to grid. In this paper, a micro inverter with PI and fuzzy based boost converter approach is presented which enables the designer to make use of the boost converters advantages, while improving the control difficulties. This control method allows the selection of passive components predominantly based on ripple and reliability specifications while requiring only one state reference signal. This method becomes smaller and more reliable.

Keywords: Photovoltaic array, Modeling, Grid-connected photovoltaic system, MPPT control, Power inverter.

I. INTRODUCTION

The much concerned with the fossil fuel exhaustion and the environmental problems are caused by the conventional power generation. Nowadays, renewable energy sources, such as photovoltaic (PV) panels and wind-generators, are now widely used. PV systems are the most direct way to convert solar radiation into electricity and are based on the PV effect, which was first observed by Henri Becquerel in 1839. It is quite generally defined as the emergence of an electric voltage between two electrodes attached to a solid or liquid system upon shining light onto this system. Practically, all PV devices incorporate a PN junction in a semiconductor across which the photo voltage is developed [1-2]. These devices are also known as solar cells. Light absorption occurs in a semiconductor material. The Semiconductor material has to be able to absorb a large part of the solar spectrum [3].

The PV generation is gaining increased importance as a renewable source. It is used today in many applications e.g. battery charging; water pumping, home power supply, swimming-pool heating systems, satellite power systems.... The PV systems have the advantage of being maintenance and pollution-free but their installation cost is high and, in most applications; they require a power conditioner (DC/DC or DC/AC converter) for load interface. Since PV modules still have relatively low conversion efficiency. The overall system cost can be reduced using high efficiency power conditioners which, in addition, are designed to extract the maximum possible power from the PV module [4-7].

The PV generators exhibit non-linear I-V characteristics. On the other hand, the optimum operating point changes with the solar irradiation, and cell temperature [8]. Therefore, online tracking of the maximum power point of a PV array is an essential part of any successful PV system. A variety of maximum power point tracking (MPPT) methods is developed in literature. For example, in [9] a MPPT is implemented with a boost converter the Incremental Conductance algorithm, is based on the principle that the slope of the PV array power curve is zero at the maximum power point.

The increasing of the world energy demand, due to the modern industrial society and population growth, is motivating a lot of investments in alternative energy solutions, in order to improve energy efficiency and power quality issues. The use of photovoltaic energy is considered to be a primary resource, because there are several countries located in tropical and temperate regions, where the direct solar density may reach up to 1000 W/m². At present, photovoltaic (PV) generation is assuming increased importance as a renewable energy sources application because of distinctive advantages such as simplicity of allocation, high dependability, absence of fuel cost, low maintenance and lack of noise and wear due to the absence of moving parts [10].

The cell conversion ranges vary from 12 percentage of efficiency up to a maximum of 29 percentages for very expensive units [11]. In spite of those facts, there has been a trend in price decreasing for modern power electronics systems and photovoltaic cells, indicating good promises

for new installations. However, the disadvantage is that photovoltaic generation is intermittent, depending upon weather conditions. Thus, the MPPT makes the PV system providing its maximum power and to help get stable and reliable power from PV system for both loads and utility grid, and thus improve both steady and dynamic behaviors of the whole generation system [12]. In this paper I have studied a grid-connected photovoltaic generation system which is composed of PV array, power electronic converters, filter, controllers, local loads and utility grid as shown in figure

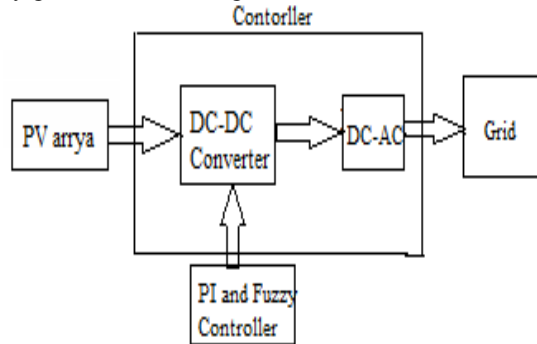


Fig 1: Block diagram of grid connected PV system.

The block diagram representation of grid connected PV system is given in figure.1. In this PV array is connected to dc-dc converter. The switching pulses for dc-dc converter is generated by fuzzy logic control based MPPT and gate generator arrangement. By using feedback voltage and power taken from the PV array, fuzzy logic control based MPPT produces a reference for the converter and using this reference, PWM generator produces switching signal for the dc-dc converter. These reference signals are given to sinusoidal PWM generator which produces six switching pulses for the inverter. The overall system uses a high efficiency fuzzy logic control based MPPT and buck converter, produces PV array voltage corresponding to the maximum power. The three phase inverter with P-Q control and LC filter produces sinusoidal ac voltage and current having less THD.

II. SIMULATION MODELS

Modeling and simulating PV power systems are investigated in this section. By default, all symbols that are used in equations refer to the definition table shown in the Nomenclature.

A. Modeling Photovoltaic Cells

The ideal single-diode model (ISDM) which is shown in Fig.2 was proposed to represent PV outputs for crystalline-based solar cells. The simplified model shows computational efficiency but provides fewer tuning parameters in comparison with the standard single-diode model that was presented in [1]–[3]. The model parameters should be properly identified, and the modeling accuracy should be evaluated carefully before it

is integrated into system simulation. The I–V characteristic for an ISDM is expressed as

$$i_{PV} = i_{ph} - i_s \left[e^{\left(\frac{qV_{PV}}{kATC} \right)} - 1 \right] \quad (1)$$

The definition of variables and constants in (1) refers to the nomenclature table. A is an unknown parameter that needs to be identified. Since the prior work in did not give a clear illustration for parameter extraction and simulation construction, the parameterization and model implementation are shown in the following sections.

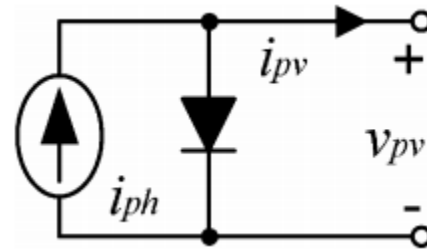


Fig. 2. Equivalent circuit for the ideal single-diode PV-cell model.

B. Photovoltaic Model Parameterization

PV manufacturers provide the values of open-circuit voltage (VOCS), short-circuit current (ISCS), and the maximum power point (VMPP, IMPP) at STC. According to the equivalent circuit of ISDM, the value of the photon current i_{ph} is equal to that of the short-circuit current ISCS at STC. When the solar cell is open-circuited, the output current of a PV cell is zero. Therefore, the I–V characteristics at STC can be expressed as

$$I_{SS} = \frac{I_{SCS}}{e^{\left(\frac{qV_{OCS}}{kATCS} \right)} - 1} \quad (2)$$

At the MPP of STC, the I–V characteristic equation can be expressed as

$$I_{MPP} = I_{SCS} - I_{SS} \left[e^{\left(\frac{qV_{MPP}}{kATCS} \right)} - 1 \right] \quad (3)$$

Therefore, the ideality factor A can be derived from (4), shown below, by the substitution of (2) into (3):

$$\frac{e^{\frac{qV_{MPP}}{kATCS}} - 1}{e^{\frac{qV_{OCS}}{kATCS}} - 1} = 1 - \frac{I_{MPP}}{I_{SCS}} \quad (4)$$

The diode saturation current I_{SS} can be found by applying A back to (2). Thus, the I–V characteristics at STC can be expressed as (5), shown below, where the photon current and saturation current are constant:

$$i_{PV} = I_{SCS} - I_{SS} \left[e^{\left(\frac{q v_{PV}}{k A T_{CS}} \right)} - 1 \right] \quad (5)$$

C. Photovoltaic Model Construction for Simulation

Both the photon current and saturation current change with the solar radiation and cell temperature. For the irradiance deviated from STC, the expression of i_{ph} can be written as

$$i_{ph}(E_e, \Delta T) = \frac{E_e}{E_{STC}} I_{SCS} (1 + \alpha_T \Delta T) \quad (6)$$

Where the definitions of E_e and E_{STC} refer to the nomenclature table. ΔT is the temperature difference between the cell temperature T_C and the STC temperature T_{CS} , and α_T is the current temperature coefficient that is given by the product datasheet. The expression in (6) shows that the photon current varies with both solar irradiance and cell temperature. The open-circuit voltage can be derived as

$$V_{OC}(\Delta E_e, \Delta T) = V_{OCS} (1 + \beta_T \Delta T) (1 + \gamma_E \Delta E_e) \quad (7)$$

Where the definitions of β_T and γ_E , and E_e and E_{STC} refer to the nomenclature. ΔE_e is the irradiance difference from the STC , and β_T is given by the product datasheet. The irradiance coefficient on voltage γ_E can be determined from the evaluation of the I-V curves for various insulation levels. For example, the open-circuit voltage is given as $V_{OC0.8}$, when the irradiance is 0.8 kW/m^2 , and the cell temperature is 25°C . The value of γ_E can be estimated as

$$\gamma_E = \left(\frac{V_{OC0.8}}{V_{OCS}} - 1 \right) / (1 - 0.8) \quad (8)$$

Therefore, the diode saturation current can be updated by following the environmental variation, which is shown as

$$i_s(\Delta E_e, \Delta T) = \frac{i_{ph}(E_e, \Delta T)}{e^{\left[\frac{q V_{OC}(\Delta E_e, \Delta T)}{k A (T_{CS} + \Delta T)} \right]} - 1} \quad (9)$$

The I-V characteristic equation can be written as (10), shown below, corresponding to the variation of the solar irradiance and cell temperature

$$i_{PV} = i_{ph}(E_e, \Delta T) - i_s(\Delta E_e, \Delta T) \left[e^{\left(\frac{q v_{PV}}{k A (T_{CS} + \Delta T)} \right)} - 1 \right] \quad (10)$$

D. Terminal Output Implementation

The single-cell model can be aggregated to any size of a PV array, as shown in Fig.3. N_s and N_p are the numbers of cells that are connected in series and parallel, respectively. When the mathematical representation is combined with a controllable current resource, the model gives terminal outputs regarding to voltage and current V_{pv} and I_{pv} which are compatible with the majority of off-the-shelf circuit-based simulation tools, such as the

SimPowerSystems for Simulink, PSIM, PSPICE, PSCAD, etc. The equation, i.e., $i_{pv} = f(v_{pv}, E_e, \Delta T)$, is updated every simulation step following (10) and operating variation. A generalized simulation flowchart is illustrated in Fig.4.

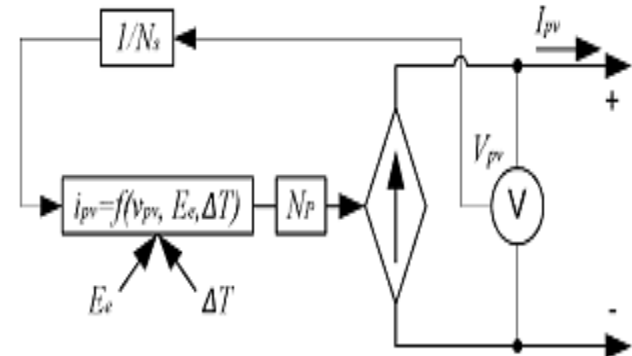


Fig.3. Block diagram of the PV array aggregation and the interconnection interface applicable for commercial simulation software.

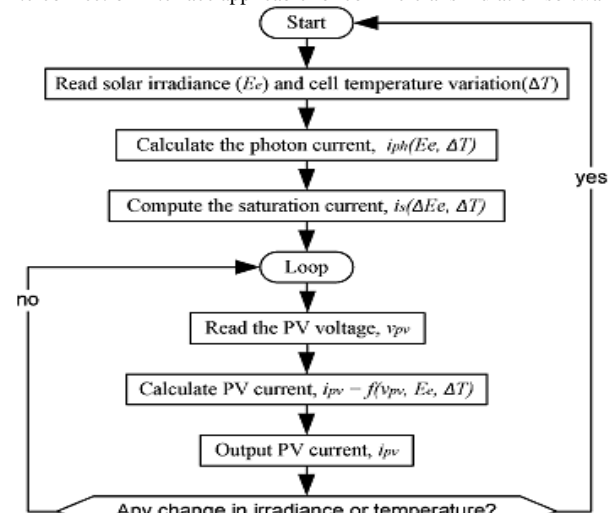


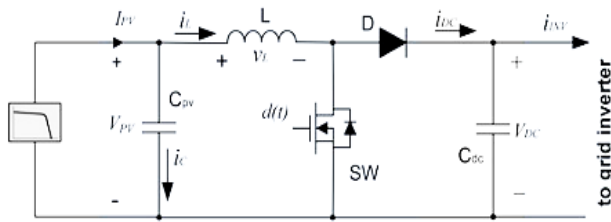
Fig.4. Flowchart of the PV model simulation.

Unlike the proposed PV model in [1]–[3], the simplified model ignores the coupled terms between i_{pv} and v_{pv} . E_e and ΔT are the environmental variables. The value of v_{pv} is determined by the power equilibrium between the PV generation and load, which is regulated by the interconnected power interface. Therefore, a more efficient simulation can be expected since no iterative solver is needed.

E. Interfacing with Intermediate DC Link

For two-stage conversion topologies, as shown in Fig.1 (a), the non-isolated dc/dc boost topology is commonly used as the PV front-end power converter (PVFEC) because of the voltage step-up requirement and its simplicity. The control of the PVFEC is the MPPT. One study indicates that the boost topology is superior over the buck in terms of cheaper implementation and better dynamics. The circuit diagram can be depicted as Fig.5,

where the PV-array model refers to the diagram in Fig. 2, and the IDCL capacitor C_{dc} is the joint connection to dc/ac inverter.



PV array model MPPT power interface DC link
Fig.5. Circuit schematics showing the combination of the PV array and the dc/dc power interface.

Averaged models show advantages of fast simulation if the system switching harmonics are not concerned. This feature is important to simulate a large power system with multiple inverter-based generators. Assuming that the dc/dc converter works in continuous conduction mode (CCM), the averaged model can be derived as

$$\left. \begin{aligned} C_{PV} \frac{dV_{PV}}{dt} &= I_{PV} - i_L \\ L \frac{di_L}{dt} &= V_{PV} - (1-d)V_{dc} \\ C_{dc} \frac{dV_{dc}}{dt} &= i_{dc} - i_{INV} \end{aligned} \right\} \Rightarrow \begin{cases} V_{PV} = \frac{1}{C_{PV}} \int (I_{PV} - i_L) dt \\ i_L = \frac{1}{L} \int [V_{PV} - (1-d)V_{dc}] dt \\ V_{dc} = \frac{1}{C_{dc}} \int ((1-d)i_L - i_{INV}) dt \end{cases} \quad (11)$$

Following the expression in (11), the averaged model can be constructed as shown in Fig.6, where the input variable is the injection current to the grid inverter i_{INV} , the control variable is the duty cycle d , and the state variables include V_{dc} , V_{PV} , and i_L . The environmental inputs that comprise E_c , and ΔT affect the PV-array model output. For the presented two-stage power conversion with IDCL, the values of d and i_{INV} are determined by the MPPT function and V_{dc} regulation, respectively.

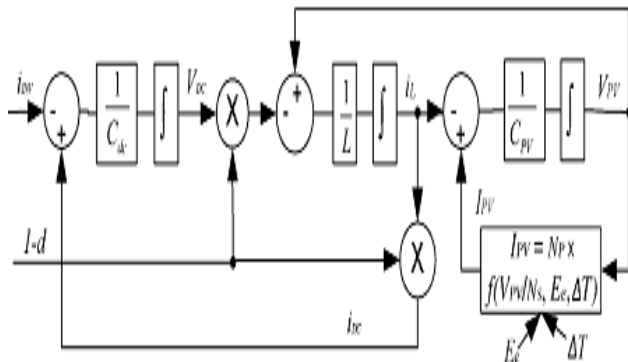


Fig.6. Implementation of the averaged model in CCM combining the PV array and the boost converter power interface.

The output power of dc/ac grid inverters P_{ac} can be estimated as (12), shown below, where the conversion efficiency η can be determined by (13), shown below, applying the peak conversion Efficiency η_{max} and the self-power consumption P_{self}

$$P_{ac} = \eta P_{pv} \text{ or } P_{ac} = \eta V_{pv} I_{pv} \quad (12)$$

$$\eta = \frac{(P_{pv} - P_{self}) \times \eta_{max}}{P_{pv}} \quad (13)$$

P_{self} is accumulated power loss that results from microcontrollers, drive circuits, human machine interfaces, other accessories, etc. Since the grid-side voltage is known and steady, the RMS value of the ac injection current can be calculated.

F. Interfacing with Grid without IDCL

String inverters show significant generation degradation that results from PV module mismatch and partial shading. The emerging solution is the MIC, which is also called the micro inverter, to eliminate the power loss that results from inconsistent impacts. A specific MIC, which is shown in Fig.7 and adopting the interleaved fly back topology, is considered in this study. The topology offers the advantages of high efficiency, reliability, power sharing, galvanic isolation, and reduced PV voltage ripple. Therein, all the details about the converter operation can be found.

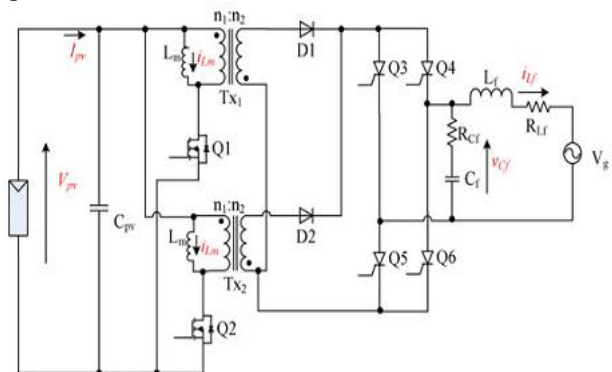


Fig.7. Topology of the interleaved fly back MIC for solar grid-tied systems.

The simulation model of the MIC is developed by the averaging technique. The model diagram is shown in Fig.8, where D represents the duty cycle, and $D1$ is defined as $1-D$. The fourth-order dynamic system includes four state variables, v_{pv} , v_{Cf} , i_{Lf} , and i_{Lm} , which result from the input and output storage units and illustrated in the shadowed boxes. In Fig.3.8, the boxes with broken lines represent the system inputs, and the duty cycle D is the control variable. The variables V_{pv} and I_{pv} are associated

with the PV-panel model, which is presented in Section II.

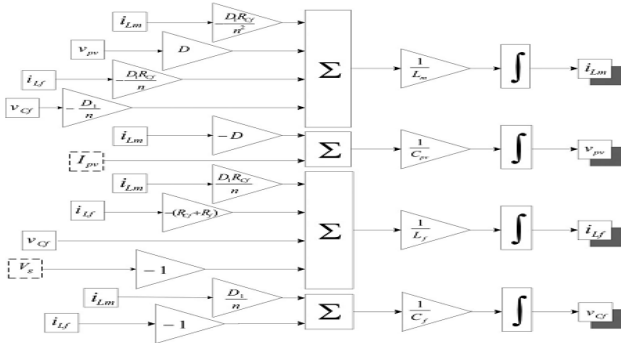


Fig.8. Averaged simulation model of the fly back-based MIC with current unfolding circuit.

G. Dynamic Model of Maximum Power Point Tracking

The voltage of the optimal operating point (VOOP) is the index that represents the MPP. In this study, it is estimated as

$$V_{OOP}(\Delta E_e, \Delta T) = V_{MPP}(1 + \beta_T \Delta T)(1 + \gamma_E \Delta E_e) \quad (14)$$

Where the definitions of β_T and γ_E refer to the nomenclature table. ΔE_e is the irradiance difference from the STC. The temperature coefficient can be directly obtained from the product datasheet. The irradiance coefficient on voltage can be determined the evaluation of I-V curves that are based on various insolation levels.

One of the commonly used MPPT algorithms is the perturbation and observation (P&O) method, which applies two parameters, the perturbation time interval ΔT MPPT and perturbation amplitude ΔT . Thus, the MPP tracking dynamics are implemented by a slew-rate limiter, as expressed in (15), shown below, which defines the maximum rate of the set point change.

$$SR = \frac{\Delta V}{\Delta T_{MPPT}} \quad (15)$$

As a result, the MPPT operation can be simplified as the diagram shown in Fig.9, where the optimal operating point is calculated by (14), and the slew-rate limiter mimics the MPP tracking dynamics.

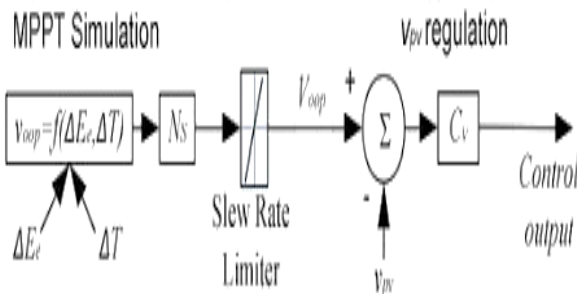


Fig.9. Proposed simulation implementation of MPPT dynamics using a slew rate limiter.

III. FUZZY LOGIC CONTROL

L. A. Zadeh presented the first paper on fuzzy set theory in 1965. Since then, a new language was developed to describe the fuzzy properties of reality, which are very difficult and sometime even impossible to be described using conventional methods. Fuzzy set theory has been widely used in the control area with some application to power system [5]. A simple fuzzy logic control is built up by a group of rules based on the human knowledge of system behavior. Matlab/Simulink simulation model is built to study the dynamic behavior of converter. Furthermore, design of fuzzy logic controller can provide desirable both small signal and large signal dynamic performance at same time, which is not possible with linear control technique. Thus, fuzzy logic controller has been potential ability to improve the robustness of compensator.

The basic scheme of a fuzzy logic controller is shown in Fig.10 and consists of four principal components such as: a fuzzy fication interface, which converts input data into suitable linguistic values; a knowledge base, which consists of a data base with the necessary linguistic definitions and the control rule set; a decision-making logic which, simulating a human decision process, infer the fuzzy control action from the knowledge of the control rules and linguistic variable definitions; a de-fuzzification interface which yields non fuzzy control action from an inferred fuzzy control action [10].

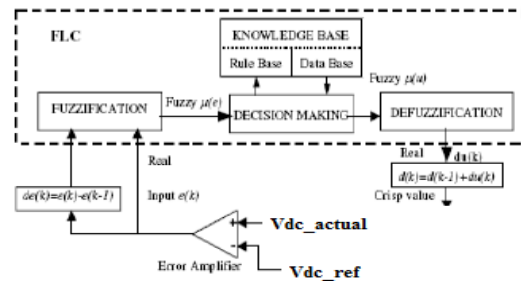


Fig.10. Block diagram of the Fuzzy Logic Controller (FLC) for Proposed Converter.

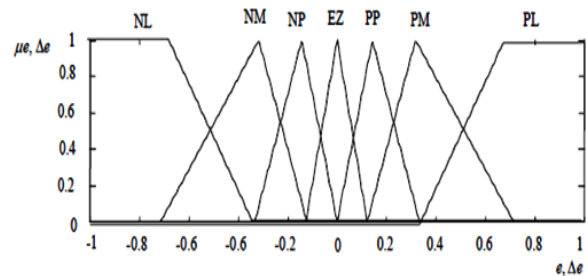


Fig.11. Membership functions for Input, Change in input, Output.

Rule Base: the elements of this rule base table are determined based on the theory that in the transient state, large errors need coarse control, which requires coarse input/output variables; in the steady state, small errors need fine control, which requires fine input/output variables.

Based on this the elements of the rule table are obtained as shown in Table, with 'Vdc' and 'Vdc-ref' as inputs

Δe \ e	NL	NM	NS	EZ	PS	PM	PL
NL	NL	NL	NL	NL	NM	NS	EZ
NM	NL	NL	NL	NM	NS	EZ	PS
NS	NL	NL	NM	NS	EZ	PS	PM
EZ	NL	NM	NS	EZ	PS	PM	PL
PS	NM	NS	EZ	PS	PM	PL	PL
PM	NS	EZ	PS	PM	PL	PL	PL
PL	NL	NM	NS	EZ	PS	PM	PL

IV.MATLAB/SIMULATION RESULTS

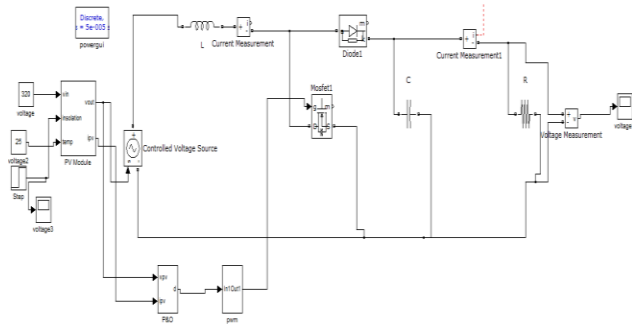


Fig. 12. Matlab/Simulink model of solar irradiance for Converter.

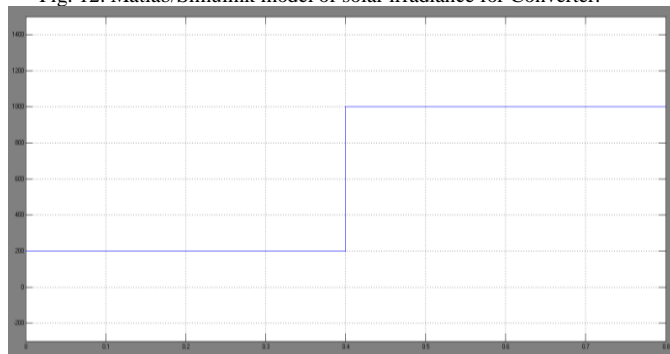


Fig.12.solar irradiance of PV systems.

Fig. 12 shows that the proposed estimation follows the same dynamic as the P&O operation, but neglects the perturbation ripples and the sudden overshoot of PV voltage that is caused by the step irradiance change from 20% to 100%.

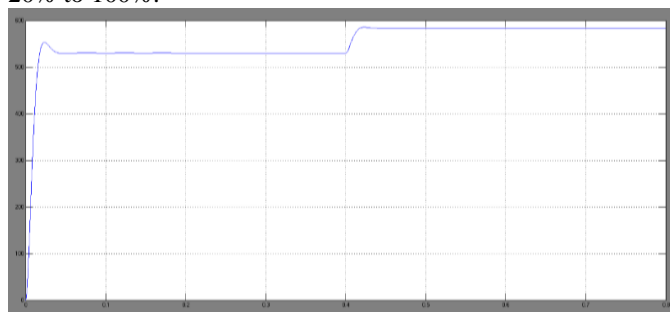


Fig. 13. Solar irradiance impact on the voltage.

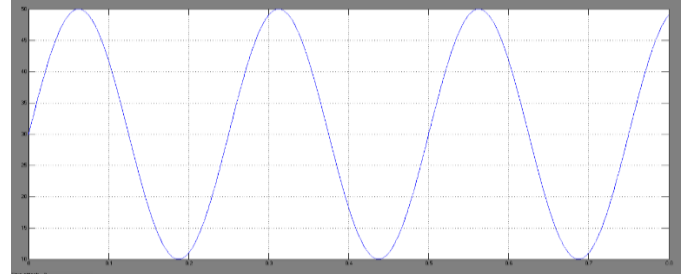


Fig.14.Temperature changes from PV system.

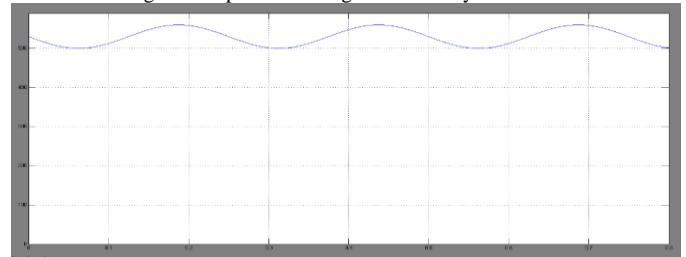


Fig. 15. Temperature effect on the voltage of optimal operating point.

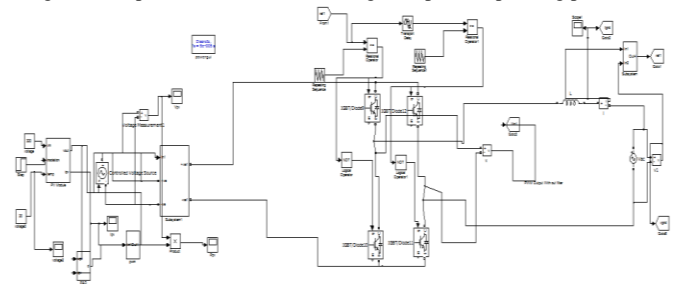
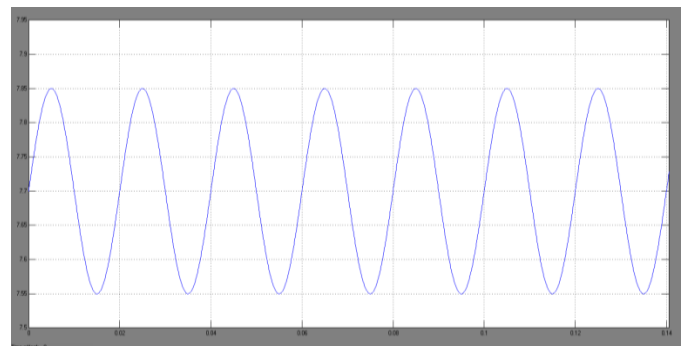
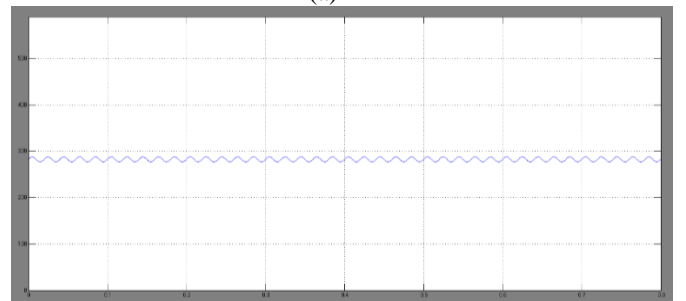


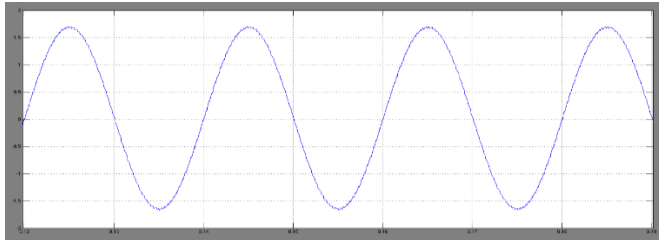
Fig.16.Matlab/Simulatin model of the combination of the PV array and the dc/dc power interface.



(a)

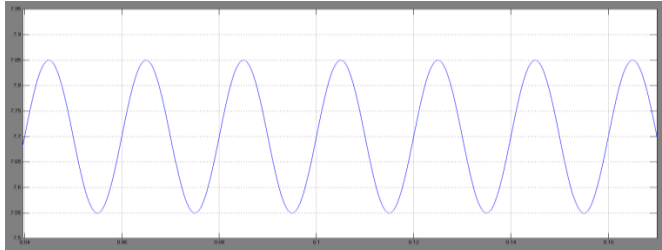


(b)

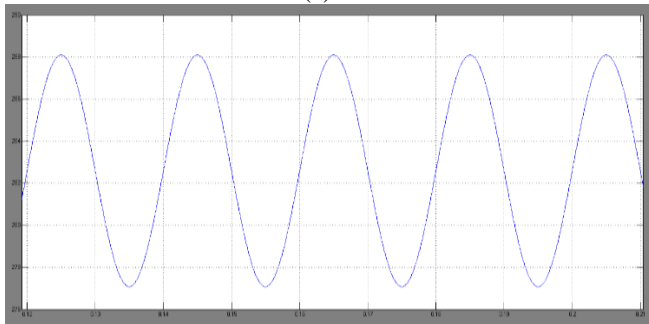


(c)

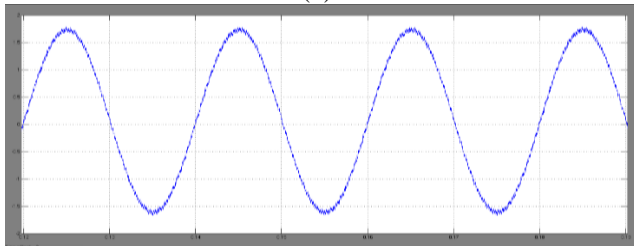
Fig. 17. Simulated waveforms generated by the proposed MIC model including (a) PV current, (b) ac output current and (c) PV power.



(a)



(b)



(c)

Fig. 18. Simulated waveforms generated by the proposed physical model including (a) PV current, (b) ac output current, and (c) PV power.

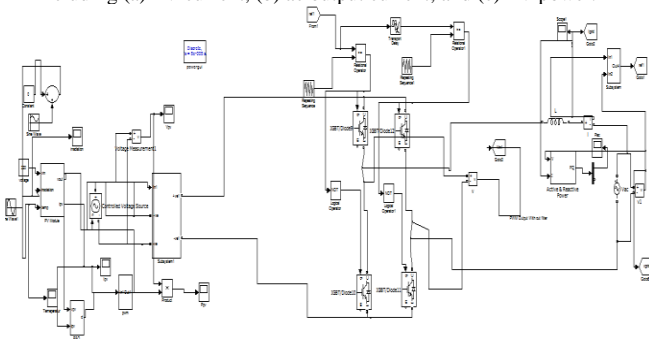


Fig.19. Matlab/Simulation model of the interleaved fly back MIC for solar grid-tied systems.

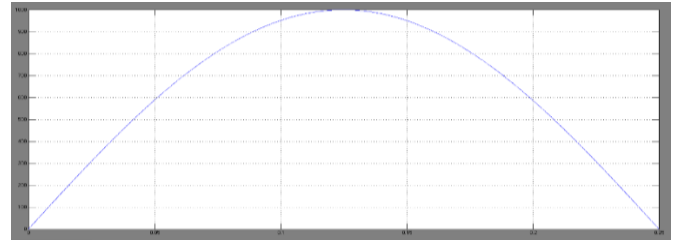


Fig.20.solar irradiance.

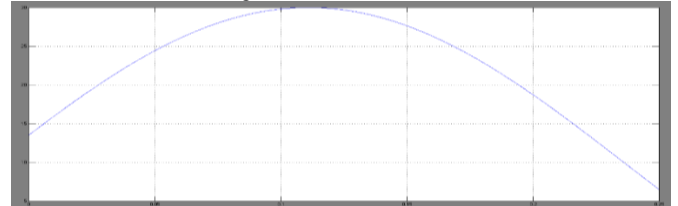


Fig.21.solar temperature.

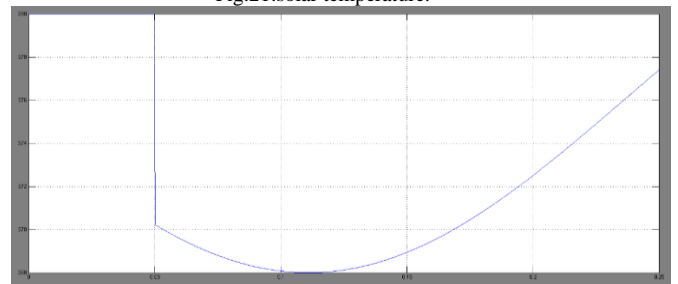


Fig.22.PV voltage.

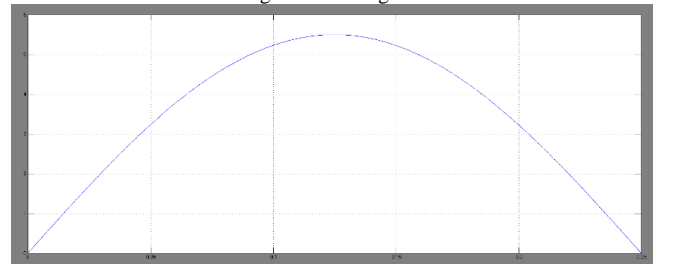


Fig.23.PV Current.

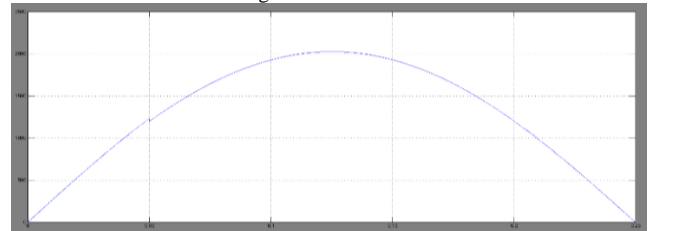


Fig.24.PV Power.

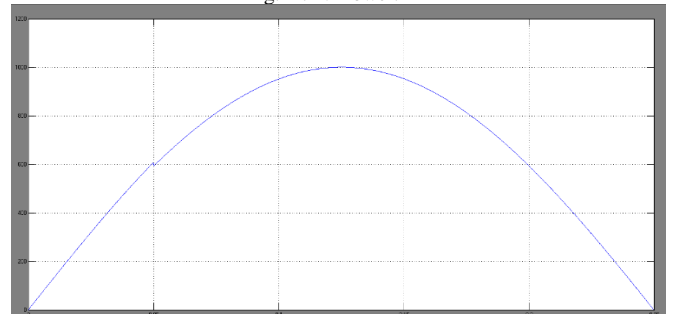


Fig.25.grid side power.

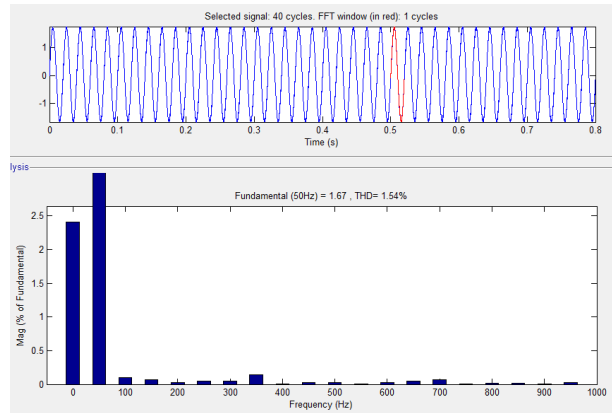


Fig.26.Current THD with PI controller.

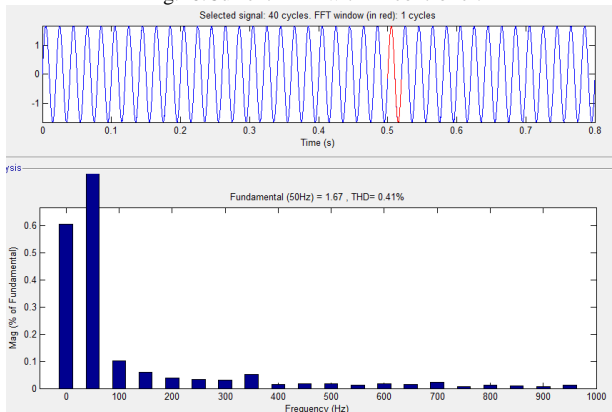


Fig.27.Current THD with Fuzzy logic controller.

V.CONCLUSION

This paper presents a technique to design and control of grid-connected PV generation system, identify its components, and describe how it works. In order to convert the solar energy efficiently, the MPPT algorithm for photovoltaic systems based on P&O algorithm has been presented. It should be tracked to ensure the PV array to generate most power to utility grid, and describe the following control algorithms used for the inverter DC-AC for regulate active and reactive power sat connection bus. This paper has presented a general approach to modeling and simulating PV power systems with regard to electrical engineering perspectives. A simplified PV model is developed showing the detailed parameterization, which is based on the given information of the manufacturer datasheet. Since the majority of PV power system is grid-tied, the modeling process focuses on two common power interfaces that include the two stage power conversion with IDCL and single-stage conversion without IDCL. The MIC that is called “micro inverter” is also included for the simulation study. Detailed model of grid-connected photovoltaic generation system components, in MATLAB /Simulink software was done. Fuzzy controlled MPPT strategy is used for PV output voltage to achieve closed loop control which can

smoothly and quickly track the maximum power point of PV array.

REFERENCES

- [1] M. G. Villalva, J. R. Gazoli, and E. R. Filho, “Comprehensive approach to modeling and simulation of photovoltaic arrays,” *IEEE Trans. Power Electron.*, vol. 24, no. 5, pp. 1198–1208, May 2009.
- [2] F. Caracciolo, E. Dallago, D. G. Finarelli, A. Liberale, and P. Merhej, “Single-variable optimization method for evaluating solar cell and solar module parameters,” *IEEE J. Photovoltaic’s*, vol. 2, no. 2, pp. 173–180, Apr. 2012.
- [3] A. Ortiz-Conde, D. G. Lugo-Muñoz, and F. J. Garcí’a-Sánchez, “An explicit multiexponential model as an alternative to traditional solar cell models with series and shunt resistances,” *IEEE J. Photovoltaics*, vol. 2, no. 3, pp. 261–268, Jul. 2012.
- [4] D. Sera, R. Teodorescu, and P. Rodriguez, “PV panel model based on datasheet values,” in *Proc. IEEE Int. Symp. Ind. Electron.*, 2007, pp. 2392–2396.
- [5] A. N. Celik and N. Acikgoz, “Modelling and experimental verification of the operating current of mono-crystalline photovoltaic modules using four- and five-parameter models,” *Appl. Energy*, vol. 84, pp. 1–15, 2007.
- [6] W. D. Soto, S. A. Klein, and W. A. Beckman, “Improvement and validation of a model for photovoltaic array performance,” *Sol. Energy*, vol. 80, pp. 78–88, 2006.
- [7] S. Liu and R. A. Dougal, “Dynamic multiphysics model for solar array,” *IEEE Trans. Energy Convers.*, vol. 17, no. 2, pp. 285–294, Jun. 2002.
- [8] J. A. Gow and C. D. Manning, “Development of a photovoltaic array model for use in power-electronics simulation studies,” *IEE Proc. Electr. Power Appl.*, vol. 146, no. 2, pp. 193–200, Mar. 1999.
- [9] M. A. Hamdy and R. L. Call, “The effect of the diode ideality factor on the experimental determination of series resistance of solar cells,” *Sol. Cells*, vol. 20, pp. 119–126, 1987.
- [10] P. Minwon and Y. In-Keun, “A novel real-time simulation technique of photovoltaic generation systems using RTDS,” *IEEE Trans. Energy Convers.*, vol. 19, no. 1, pp. 164–169, Mar. 2004.
- [11] N. D. Kaushika and N. K. Gautam, “Energy yield simulations of interconnected solar PV arrays,” *IEEE Trans. Energy Convers.*, vol. 18, no. 1, pp. 127–134, Mar. 2003.
- [12] M. Veerachary, “PSIM circuit-oriented simulator model for the nonlinear photovoltaic sources,” *IEEE Trans. Aerosp. Electron. Syst.*, vol. 42, no. 2, pp. 735–740, Apr. 2006.